

Re-examination of C₁–C₅ alkyl nitrates in Hong Kong using an observation-based model



X.P. Lyu^a, Z.H. Ling^{a,b}, H. Guo^{a,*}, S.M. Saunders^c, S.H.M. Lam^{c,d}, N. Wang^a, Y. Wang^a, M. Liu^a, T. Wang^a

^a Department of Civil and Environmental Engineering, The Hong Kong Polytechnic University, Hong Kong

^b Department of Atmospheric Science, School of Environmental Science and Engineering, Sun Yat-sen University, China

^c School of Chemistry and Biochemistry, University of Western Australia, Perth, Western Australia, Australia

^d Pacific Environment Limited, Perth, Western Australia, Australia

HIGHLIGHTS

- Both PMF and MCM explored the pathways to RONO₂.
- CH₃O + NO₂ was not the major pathway to MeONO₂.
- RONO₂ formation made negative contribution to O₃.
- Nitrogen partitioning in RONO₂ was quantified.

ARTICLE INFO

Article history:

Received 17 April 2015

Received in revised form

15 July 2015

Accepted 10 August 2015

Available online 29 August 2015

Keywords:

Alkyl nitrate

Photochemical formation

O₃ production

PBM-MCM model

Field observation

ABSTRACT

The photochemical formation of alkyl nitrates (RONO₂) and their impact on ozone (O₃) formation were investigated using a Photochemical Box Model incorporating the Master Chemical Mechanism (PBM-MCM). The model was constrained with field measurement data collected on selected O₃ episode days at Tai O, a rural-coastal site in southwestern Hong Kong, from August 2001–December 2002. The in-situ observations showed that the sum of C₁–C₅ RONO₂ varied from 30.7 ± 14.8 pptv in spring to 120.7 ± 10.4 pptv in autumn, of which 2-butyl nitrate dominated with the highest average concentration of 30.8 ± 2.6 pptv. Model simulations indicated that the pathway of CH₃O reacting with NO₂, proposed in our previous study, made minor contributions (11.3 ± 0.7%) to methyl nitrate formation. Indeed, 51.8 ± 3.1% and 36.5 ± 6.3% of the methyl nitrate was attributed to the reaction of CH₃O₂+NO and to oceanic emissions/biomass burning, respectively. For the C₂–C₅ alkyl nitrates, the contribution of photochemical formation increased with increasing carbon number, ranging from 64.4 ± 4.0% for ethyl nitrate (EtONO₂) to 72.6 ± 4.2% for 2-pentyl nitrate (2-PenONO₂), while the contribution of oceanic emissions/biomass burning decreased from 35.1 ± 6.5% for EtONO₂ to 26.8 ± 6.8% for 2-PenONO₂. Model simulations of photochemical O₃ levels influenced by RONO₂ chemistry showed that the formation of methyl-, ethyl-, *i*-propyl-, *n*-propyl-, 2-butyl-, 2-pentyl-, and 3-pentyl-nitrates led to O₃ reduction of 0.05 ± 0.03, 0.05 ± 0.03, 0.06 ± 0.02, 0.02 ± 0.02, 0.18 ± 0.04, 0.09 ± 0.02 and 0.06 ± 0.02 ppbv, respectively, with an average reduction rate of 11.0 ± 3.2 ppbv O₃ per 1 ppbv RONO₂ formation. The C₁–C₅ RONO₂ constituted 18.6 ± 1.9% of the entire RONO₂, and had a nitrogen reserve of 4.1 ± 0.2%, implying their potential influence on O₃ production in downwind areas.

© 2015 Elsevier Ltd. All rights reserved.

1. Introduction

Photochemical pollution characterized by elevated O₃ in the

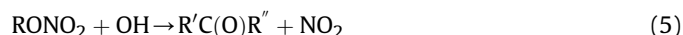
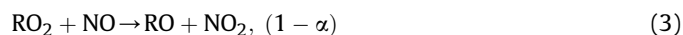
troposphere (Guo et al., 2013a; Wang et al., 2009) is of increasing concern in megacities, such as the city cluster in the Pearl River Delta (PRD) region, where huge emissions of O₃ precursors, *i.e.*, volatile organic compounds (VOCs) and nitrogen oxides (NO_x) from industries and traffic have caused intense periods of high photochemical O₃ formation (Cheng et al., 2010; Ling et al., 2011) notably

* Corresponding author.

E-mail address: ceguohai@polyu.edu.hk (H. Guo).

in the autumn period. Alkyl nitrates (RONO_2) are formed as byproducts in the process of O_3 formation, and are also temporary reservoirs of nitrogen. However, to date there have been few studies on the influence of individual alkyl nitrate on the O_3 budget (Wang et al., 2013; Williams et al., 2014).

There are 5 key gas phase reactions in the troposphere, (1)–(5), for the production and destruction of alkyl nitrates:



The photochemical formation of RONO_2 is mainly attributed to reactions (1) and (2) (Atkinson et al., 1982; Wang et al., 2013). Alternative pathways, *i.e.*, reactions between organic aerosols and particle-phase nitrates, and NO_3 initiated oxidation of RO_2 at nighttime, also contribute to photochemical RONO_2 production (Worton et al., 2010). Studies (Jenkin and Clementshaw, 2000; Suarez-Bertoa et al., 2012) indicate that reaction (1) contributes most to ambient RONO_2 and becomes increasingly important with increasing carbon number of the RO_2 species, because the decomposition rate of the vibrationally-excited RONO_2 decreases with increased complexity of the alkyl (R) group, hence the survival of stabilized RONO_2 increases (Atkinson et al., 1983). If the vibrationally-excited RONO_2 is not formed, an oxygen atom (O) exchange between RO_2 and NO will occur, *i.e.*, reaction (3). The branching ratio (α) is often used to define the relative reactivity of reaction (1) competing with the reaction (3) (Flocke et al., 1998; Farmer et al., 2011). In contrast to the formation pathway of reaction (1), the production efficiency of RONO_2 from reaction (2), *i.e.*, $\text{RO} + \text{NO}_2$, decreases with increasing carbon number because of the increasing tendency of isomerization and decomposition of RO, and relatively lower abundance of RO compared to the methoxy radical (CH_3O) as the carbon number increases (Atkinson et al., 1982; Williams et al., 2014).

As well as photochemical formation, equatorial oceans (Atlas et al., 1993; Blake et al., 2003) are a primary source of ambient RONO_2 , particularly for light ($< \text{C}_2$) RONO_2 . Blake et al. (2003) reported that methyl nitrate (MeONO_2) was significantly emitted from tropical and subtropical oceans, which was an important source of excess MeONO_2 that cannot be explained by photochemical formation. Additionally, biomass burning is also a source of RONO_2 , for which Simpson et al. (2002) proposed a formation mechanism in the combustion stage involving the combination of RO_2 to generate RO and the reaction of RO with NO_2 .

Since RONO_2 are formed simultaneously with O_3 , they are good tracers of photochemical pollution (Simpson et al., 2006; Aruffo et al., 2014). They also affect O_3 production by interfering with the NO_x budget as temporary nitrogen reservoirs (Aruffo et al., 2014). The availability of reactive nitrogen will be reduced through reactions (1) and (2) due to the long atmospheric lifetimes of RONO_2 (Atlas, 1988). Moreover, the RO generated from reaction (3) decreases, resulting in the loss of OH and HO_2 . These will reduce the potential for O_3 production. On the other hand, the formation of RONO_2 competes with the reaction of O_3 titration by NO. As a temporary reservoir of reactive NO_x , RONO_2 can also release RO and NO_2 through photolysis (reaction (4)) and OH-initiated oxidation (reaction (5)) (Aschmann et al., 2011; He et al., 2011). The additional

NO_2 , secondary organic degradation products (*i.e.*, PANs, aldehydes, ketones, etc.) and radicals (*i.e.*, RO_2 , HO_2 , OH, etc.) consequently promote the photochemical production of O_3 . During the process of RONO_2 degradation, OH and HO_2 are consumed and their recycling is strongly dependent on the reactivity of the carbonyls generated from the oxidation of RO (Derwent et al., 2005). It remains uncertain whether RONO_2 make positive or negative contributions to O_3 formation, and what differences there are between individual alkyl nitrate species.

In this study, PBM-MCM model was adapted to investigate the photochemical formation of C_1 – C_5 RONO_2 and their impacts on O_3 production at Tai O, a rural-coastal site in southwestern Hong Kong. Using the same dataset, Simpson et al. (2006) reported the mixing ratios and seasonal patterns of the observed RONO_2 , the potential formation pathways of MeONO_2 and the correlation between the sum of C_1 – C_5 RONO_2 and O_3 . Here alternative formation pathways of MeONO_2 were examined, and the correlations between RONO_2 and O_3 were fully developed by quantifying the impacts of the C_1 – C_5 RONO_2 formation on the net O_3 production.

2. Experimental

2.1. Sample collection and chemical analysis

From 24th Aug. 2001 to 31st Dec. 2002, a multi-pollutant sampling campaign was conducted at Tai O, a rural-coastal site in southwestern Hong Kong. Fig. 1 shows the geographical location of the sampling site (22.25°N, 113.85°E). Local emissions are not predominant at this site due to the low traffic and population density. Tai O is located approximately 30 km to the west of the urban center of Hong Kong, 30 km to the east of Macau, and at the mouth of Pearl River Estuary. This site is influenced by air pollution from the PRD region, particularly enhanced in the cooler autumn-winter seasons when northeastern winds passing over the PRD region and Hong Kong urban areas dominate. Conversely, air pollution from the PRD is less evident during the prevailing summer southerly winds bringing in fresh air and diluting the air pollution. Full details about the sampling site and field campaign are available in Wang et al. (2005) and Simpson et al. (2006).

Whole air VOC samples were collected using evacuated 2-L stainless steel canisters, which were preprocessed with 10 Torr of degassed, distilled water to quench the active surface sites of the inner walls. The canisters were cleaned and evacuated following the procedures described in Simpson et al. (2006) prior to sampling. Each whole air sample was collected through a valve for 1 min to ensure that the canister was fully filled. After sampling, the canisters were shipped to the University of California, Irvine (UCI) for chemical analysis. Totally, mixing ratios of 7 C_1 – C_5 RONO_2 , 42 nonmethane hydrocarbons (NMHCs), 26 halocarbons and 3 reduced sulfur compounds were determined. Details on the analysis techniques, detection limits and quality control strategies are given in Colman et al. (2001) and Simpson et al. (2006). It is important to note that the RONO_2 were calibrated with a new scale in 2008 that applied a factor of 2.13, 1.81, 1.24, 1.17 and 1.13 to C_1 , C_2 , C_3 , C_4 and C_5 RONO_2 . This scale was provided by Atlas (University of Miami), and accepted by the analytical team (UCI) (Simpson et al., 2011).

The measurement techniques for trace gases, *i.e.*, CO, NO, NO_y , SO_2 and O_3 are fully described in Wang et al. (2003). Briefly, CO was thermally catalyzed to CO_2 , and then measured with a gas filter correlation, non-dispersive infrared analyzer (Advanced Pollution Instrumentation, Inc., Model 300); NO and NO_y were detected with a modified commercial MoO/chemiluminescence analyzer (Thermo-Environmental Instruments, Inc. (TEI), Model 42S) that converted NO_y to NO on the surface of MoO, and then NO was

Download English Version:

<https://daneshyari.com/en/article/6337295>

Download Persian Version:

<https://daneshyari.com/article/6337295>

[Daneshyari.com](https://daneshyari.com)